

# Increasing tool life and machining performance by dynamic spindle speed control along toolpaths for milling complex shape parts

Petr Vavruska<sup>a,\*</sup>, Filip Bartos<sup>a</sup>, Michal Stejskal<sup>a</sup>, Matej Pesice<sup>a</sup>, Pavel Zeman<sup>a</sup>, Petr Heinrich<sup>b</sup>

<sup>a</sup> Department of Production Machines and Equipment, Faculty of Mechanical Engineering, Czech Technical University in Prague, Technicka 4, 16607, Prague 6, Czech Republic

<sup>b</sup> KOVOSVIT MAS Machine Tools, a.s., namesti Tomase Bati 419, 39102 Sezimovo Usti, Czech Republic

## ARTICLE INFO

### Keywords:

Spindle speed  
Feed rate  
Cutting radius  
Tool life  
Point milling  
Complex shape

## ABSTRACT

This paper focuses on dynamic spindle speed and feed rate control to increase tool life and reduce machining time during milling of complex shaped parts. Machining of complex shaped surfaces is one of the most demanding machining applications, especially if the workpiece is made of difficult-to-cut material. Tool life needs to be considered during selection of cutting conditions. Both feed rate and cutting speed also have a direct effect on the resulting roughness and accuracy. When machining with tools with a circular cutting edge, such as ball or toroidal mills, the real cutting diameter of the tool changes continuously and as a result the cutting speed along the toolpath also changes continuously. Therefore a new method to compute the required spindle speed and feed rate was proposed based on the implemented kinematic parameters of a real spindle controller. In addition, a method to calculate the effective cutting radius of the tool based on the actual height of the remaining material was proposed to achieve a constant cutting speed through dynamic spindle speed control. The benefits of using the new optimization method were verified when machining a duplex stainless steel (1.4462) part. This test confirmed that the new optimization method results in a significant increase in tool life as well as a significant saving of machining time, while achieving the desired surface quality.

## 1. Introduction

Machining of parts that consist of complex shaped surfaces is one of the most demanding machining applications, especially when high quality or precision is required for the machined surface, for example for parts from the automotive, aerospace or power industries and various moulds. High demands on precision and quality often make it necessary to optimize the feed rate. Moreover, if the workpiece is made of difficult-to-cut material, tool life must be considered during selection of technological conditions, because every change in the new tool has an impact on the resulting roughness and accuracy when machining an entire surface. Both feed rate and cutting speed (among other parameters such as ap and step-over) have a direct effect on the resulting roughness and accuracy. Feed rate directly affects productivity, which, along with tool consumption, has a direct impact on the total cost of machining a part. Increasing productivity, quality and tool life are therefore some of the most important current directions for research and development in complex part machining. Ball shaped cutters (ball-end mills) are often used to finish shaped surfaces, which is the focus of

considerable research, along with point milling strategies.

During three-axis machining of complex shapes using tools with a circular cutting edge, such as ball or toroidal tools, the contact point between the tool and the workpiece is constantly moving along the cutting edge. As a result, both the actual cutting diameter and the cutting speed are continuously changing. In multi-axis machining, the lead and tilt angles also affect the actual cutting diameter of the tool and therefore also affect the cutting speed that is achieved. Fig. 1 shows three positions of the tool relative to the workpiece as examples where the cutting diameter of the tool changes and therefore the cutting speed changes too. Fig. 1 on the left shows an example of multi-axis milling with a ball-end mill, where the tool leading angle changes as the tool moves. Fig. 1 in the middle shows a ball-end mill when the tool axis is vertical and Fig. 1 on the right shows a toroidal mill also with the tool axis in a vertical position. In all these three examples, the real cutting diameter changes and in all cases the real cutting diameter is smaller than the tool diameter. The smaller the lead or tilt angle, the smaller the effective tool cutting diameter for the machining of the material, and therefore a lower cutting speed is achieved. The small effective cutting diameter and low cutting speed have a negative impact on the resulting

\* Corresponding author.

E-mail address: [p.vavruska@rcmt.cvut.cz](mailto:p.vavruska@rcmt.cvut.cz) (P. Vavruska).

<https://doi.org/10.1016/j.jmpro.2023.04.058>

Received 5 August 2022; Received in revised form 1 April 2023; Accepted 20 April 2023

Available online 25 May 2023

1526-6125/© 2023 The Authors. Published by Elsevier Ltd on behalf of The Society of Manufacturing Engineers. This is an open access article under the CC BY-NC-ND license (<http://creativecommons.org/licenses/by-nc-nd/4.0/>).

Nomenclature			
$\rho_1$	plane defined by allowance	$d_2$	equation constant
$\vec{e}$	tool axis vector	$P_{p1}$	point on the tool axis, defining the $R_{eff1}$
$\vec{m}$	cross product of the vector $\vec{n}$ and the tool motion vector	$P_{p2}$	point on the tool axis, defining the $R_{eff2}$
$\vec{n}$	part surface normal vector	$P_p$	point on the tool axis, defining the $R_{eff}$
$\alpha$	spindle acceleration [ $\text{rad/s}^{-2}$ ]	$R$	radius of the tool [mm]
$A_1$	first intersection point of the tool, $\rho_1$ and tool motion vector	$R_{eff1}$	first effective tool cutting radius by remaining material [mm]
$A_2$	second intersection point of the tool, $\rho_1$ and tool motion vector	$R_{eff2}$	second effective tool cutting radius by remaining material [mm]
$\alpha_p$	depth of cut [mm]	$R_{eff}$	effective tool cutting radius at contact point [mm]
$C_{PS}$	intersection point of vector $\vec{n}$ and $\rho_1$	$S$	spindle speed [RPM]
$C_p$	contact point between the tool and workpiece	$S_C$	center of a ball-end mill [mm]
$d_1$	equation constant	$t$	time [s]
		$T_T$	tool tip
		$V_{B_{max}}$	maximum flank wear [ $\mu\text{m}$ ]

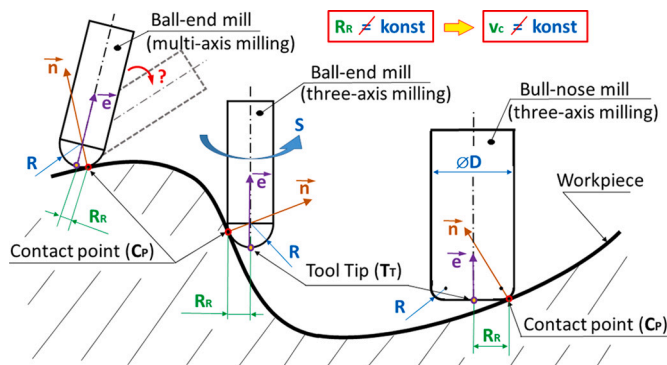


Fig. 1. Effective cutting radius during point milling.

surface quality [1]. It has also been shown that the milling strategy settings and the tool diameter have a direct effect on the resulting surface roughness [2]. Ozturk et al. [3] presented the effects caused by the lead and tilt angles on the resulting roughness of the machined surface in five-axis machining, and it was clearly shown that the lead angle and chip thickness need to be set appropriately to avoid machining on the tool tip.

Other research focuses on achieving the optimum orientation of the tool axis to the workpiece when the ball-end mill is used in combination with a specific spindle speed. This topic is addressed in paper [4], where an analysis of the factors affecting the texture of the machined surface is presented. This research showed that, when milling hardened steel with a ball-end mill for the given spindle speed range, better surface roughness is achieved with a specific lead angle than without a lead angle. Changing the lead and tilt angles of the tool, as well as the direction of milling, plays an important role when machining difficult-to-cut materials. Aspinwall et al.'s experiment [5] demonstrates the effect of cutter orientation on the machinability of Inconel 718. The orientation of the tool axis with respect to the machined surface was defined by a fixed angle of 45°. The effect of different surface row directions (pulling, pushing) was investigated and for comparison the surface was machined without setting the lead angle (three-axis milling). The experiment showed that the tooling direction and the tool axis orientation affect tool life, cutting forces and the resulting surface roughness significantly. Many researchers focus on increasing productivity by controlling feed rates.

Feng et al. [6] deals with maximizing the feed per tooth, which is determined by the just-calculated cutting force and the allowable errors/deviations of the resulting machining based on the ball-end mill

geometry and the toolpath increment. For another feed control method, a model was developed to predict spindle performance by considering different types of milling (e.g. sequential and non-sequential milling). As a result, machining time was reduced. [7] A similar topic is also presented in [8]. Tounsi et al. [9] presented an option where the feed rate is adjusted with respect to the dynamics of the machine tool movement at the calculated movement trajectory to achieve a nearly constant cutting force. The aim is to achieve smooth and precise machining. The accuracy, which is defined by the absolute deviation of the actual and theoretical target coordinates of each toolpath section, is controlled. If the distance is within the allowable deviation, the resulting cutting force is determined using a simulation model and the optimum feed rate is calculated.

Salami et al. [10] tried to generalize the cutting forces model for a ball-end mill. The aim of this research was to increase CNC machine tool productivity by optimizing the feed rate through achieving a constant cutting force for point milling strategies. Erkorkmaz et al. [11] presented a machining time reduction using feed rate control according to the tool engagement angle in the cut to maintain the specified cutting force. Wei et al. [12] proposed a discrete method for calculating cutting forces when machining shaped surfaces with ball-end mills. An advanced cutting forces model, also generalized for ball-end mills, was developed by Merdol et al. [13]. This model assumes material removal and is applicable to complex shapes of parts such as dies and moulds. By integrating the force distribution along the cutting edge, the total forces, torque, and power can be predicted using an analytical solution. The machining simulation results with the cutting forces calculation are then used to calculate new feed rates to maximize the material removal rate.

The term constant cutting speed is quite commonly used in connection with turning operations. The research in turning focuses on dynamic spindle speed control as well, especially to avoid vibrations. Al-Regib et al. [14] presented a sinusoidal characteristics to control the spindle speed for vibration avoidance (chatter) with the criterion of achieving a minimum energy level in turning operations. An improvement of the sinusoidal speed control method for suppressing self-excited vibration during turning operations with efficient energy dissipation during vibration is presented in paper [15]. Albertelli et al. [16] investigated sinusoidal spindle speed variation (sssv) on a lathe. The variation is used for chatter suppression during machining. They also measured the temperatures between the tool and part during conventional machining and spindle speed variation and presented a direct relation between cutting speed and temperature, which means that during sssv the temperature has a sine characteristic as well. This fluctuation of temperature had a negative effect on tool life. They furthermore proved that there occur different wear mechanisms when using sssv. However, in the last few years, interesting research has been

presented regarding the need to achieve a constant cutting speed even in milling operations.

The authors of [17] demonstrate the higher efficiency of machining operations in achieving a constant cutting speed with different finishing strategies and the effect on the resulting machined surface accuracy. Vavruska et al. [18] was the first to introduce a dynamic spindle speed control method for milling with a circular cutting edge tool. This paper outlines the basic benefits of this method, such as achieving higher surface quality and reducing machine time. Stejskal et al. [19] conducted an experiment on machining aluminium alloy EN AW 7075 and duplex steel DIN 1.4462 focusing on the relationship between the contact point of the ball-end mill and the actual cutting speed. They found an approximate lead angle setting range where the roughness of the machined surface starts to be sufficient and predictable. The findings led to the development of an optimization algorithm that adjusts the tool axis orientation along the toolpath.

Berthold et al. [20] investigated how spindle speed changes affect the dynamic behavior of a milling machine tool. Furthermore, they compared results from Experimental Modal Analysis (EMA) and from Operational Modal Analysis (OMA) to investigate modal behavior differences between cutting and standstill. Whereas EMA is suitable only for machine tools in idle mode, OMA is designed for machine tools that are in machining process. The excitation process selected for the OMA was a face milling process with three different spindle speed settings. The first setting was a constant spindle speed of 800 RPM, the second was a spindle speed in the range of 1000–3000 RPM and the third was a sine function spindle speed alteration. The results show that the sine spindle speed alteration is the best option for the OMA and also avoids critical frequencies during milling. Seguy et al. [21] explored spindle speed variation possibilities for high-speed milling during regenerative chatter effect. The spindle speed was altered with a given frequency and amplitude. The investigated variation functions were Sine, Triangular and Square wave. They proved that the spindle is indeed capable of such RPM changes with an error of 0.5 % to programmed value. Later, the team also proved the mathematical model for the regenerative effect for the given workpiece. They demonstrated that spindle speed variation has a positive effect on chatter suppression.

Käsemodel et al. [22] demonstrated a surface speed Optimization function for milling free-form shapes with a ball-end mill. The function takes several parameters as inputs, such as normal vector, feed per tooth, programmed cutting speed, maximum spindle speed and the previously generated NC code. Käsemodel et al. developed custom software using Visual Basic and Grasshopper to recalculate the surface speed for each machine tool position and when the RPM difference due to the effective tool diameter change was greater than 50 compared to the programmed value, they altered the NC code block with a command to set a new spindle RPM and recalculated the feed rate for that block. They also mention that the spindle speed alteration does not affect spindle life. The results show up to 30 % machining time reduction along with better surface quality and cutting force reduction. Vavruska et al. [23] proposed an optimization method, also using spindle speed control, that shows better roughness achieved in blade machining when a minimum value of the part's vibration energy is found. Vibrations often occur when machining thin-walled parts.

One way to prevent vibrations is to control the spindle speed according to the method presented by Maslo et al. [24]. Here, cutting force prediction is used simultaneously with material removal and the dynamic behavior of the workpiece is predicted by a linear parameter-varying model and the spindle speed is determined based on this model. Munoa et al. [25] also presented spindle speed control as one of the techniques for avoiding vibration during part machining. The study of dynamic parameters of part behavior and vibration suppression was addressed by Kalinski et al. [26]. A set of milling operations using a ball-end mill was presented. It was proven that the setting of the tilt angle impacts the selection of the appropriate spindle speed to achieve the best possible surface roughness. An automatic recommendation of cutting

conditions including speed to avoid chatter during roughing milling operations is presented in [27]. Based on measurement of the frequency spectrum from the audio signal (using a PDA) and the proposed algorithm, the program is able to suggest a change of cutting conditions to achieve stable machining. The machine tool operator can adopt these recommended conditions and reset the NC program accordingly.

A mathematical model that evaluates cutting speed distribution over the area of the machined surface, to which a three-axis machining operation using a ball-end mill is applied, is presented in [28]. The cutting diameter of the tool, which removes material at a given point of the toolpath, is determined using the Z-map method and then the cutting speed distribution is obtained by dividing the surface into elementary regions and calculating the average cutting speed over them. Paper [29] presents an analysis of the effects that occur when milling free-form geometric shapes with a ball-end mill. The research showed that the changing conditions at a given contact point between the tool and the workpiece surface during milling have an effect on the cutting speeds and also on the cutting force, workpiece surface quality and chip shape. By increasing the cutting speed, the area of this significant increase in cutting forces near the tool tip centre may be narrowed and the force load at all points of the shapes on the workpiece may be reduced.

Tuysuz et al. [30] present a model that predicts the cutting forces by modelling the chip thickness distribution during ball-end mill machining. An analytical model was developed considering the elastoplastic deformation of the workpiece material with respect to positive or negative rake angle of the tool. It was proven that the cutting forces increase significantly when machining the material by the tool section close to the tool tip, where the effective cutting diameter is very low and therefore the cutting speed is also very low. Batista et al. [1] experimentally verified the surface finish when machining WNr 1.2367/X38CrMoV5–3 steel with a zero tilt angle. Cycloid-shaped traces are visible on the workpiece surface which correspond to the different mechanism of the chip shearing. These cycloids have a constant pitch, which is determined by the feed rate of the tool. It is therefore evident that the technologist should set up the machining operation to avoid the area close to the tip of the ball-end mill during machining, since in this area the cutting edge is overloaded and thus the required surface roughness is not achieved, and the increased cutting forces also reduce tool life. Tool life is also the subject of the analysis in [31], where the aim is to present the effect of the tool path direction (ascending and descending) in contact with the workpiece surface on tool life. Higher vibrations were achieved in the upward machining direction than in the downward direction. Better surface roughness was achieved in the downward direction. Consequently, the high vibration in the upward machining direction caused a reduction in tool life compared to the downward machining direction.

A cutting force model that could be suitably applied to compare the variations in the setup of the technological conditions on the toolpath for ball-end mill finishing was subsequently presented in [32]. The importance of the automatic selection of the optimal technological conditions is mentioned by Sun et al. [33] In their work, they proposed a method for calculating the optimal cutting conditions for ball end mills in order to achieve the maximum volume of material removed per tooth. The computational model includes the calculation of cutting forces and prediction of machining errors and the available machine performance parameters are also among the input parameters. The research also focuses on the automatic selection of a suitable tool tilt angle with respect to the machined surface to suppress vibrations caused by tool and workpiece compliance. An algorithm that automatically orients the tool axis to avoid chatter while increasing productivity was presented in [34].

This paper aims to propose and verify a method for spindle speed control to achieve a constant cutting speed when milling complex shaped parts which take into account spindle acceleration and deceleration. This method will calculate the actual speed that a specific spindle can achieve, and thus the feed rate can be calculated to achieve a constant

feed per tooth. The paper will also present another variation of the effective cutting radius calculation. No previous work has dealt with similar approaches.

## 2. Calculation of effective cutting radius

In principle, there is more than one solution for the real effective cutting radius of the tool. The tool is in contact with material over a certain area. Therefore, there are multiple points from which the effective cutting radius may be determined. In general, two methods for calculating effective cutting radius are possible.

The first approach entails operating directly with the contact point between the tool and the workpiece and the second considers the remaining material on the workpiece in the calculation as well. The effective cutting radius determined from the contact point can be seen as  $R_{eff}$  in Fig. 2. There are essentially two possible effective cutting radius solutions determined from the intersection of the tool and the surface of the remaining material ( $R_{eff1}$  and  $R_{eff2}$ ) in the plane of cut. Both can be seen in Fig. 2 as well. The situation in the figure does not take into account the previous movement of the tool, but only indicates the relative position of the tool and the workpiece.

### 2.1. Effective cutting radius based on the contact point

This approach operates with the contact point between the tool and the workpiece. As seen in Fig. 3, the real cutting radius  $R_{eff}$  can be calculated as the distance of contact point  $C_p$  (contact point between the tool and the workpiece) from the tool axis, which is represented by unit vector  $\vec{e}$ .

The formula for calculation of the effective cutting radius is given in (1). This enables computation of the effective cutting diameter during 3-axis, 4-axis or even 5-axis machining. However, calculating the effective cutting radius based on the contact point neglects the fact that there is remaining material on the workpiece.

$$R_{eff} = |[S_c + |(C_p - S_c) \cdot \vec{e}| \cdot (-\vec{e})] - C_p| \quad (1)$$

### 2.2. Effective cutting radius based on the remaining material

The aim of the second approach is to calculate the effective cutting

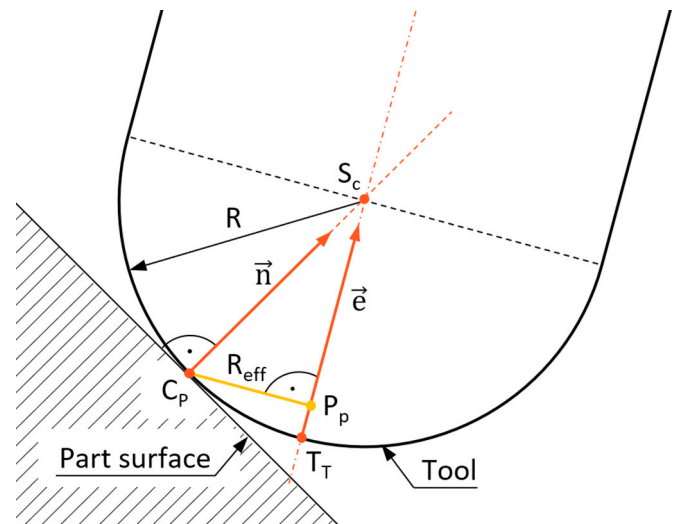


Fig. 3. Effective cutting radius given by contact point.

radius with consideration of the remaining material on the part surface during the milling operation. As already mentioned in the introduction, there are already methods of detecting material and workpiece intersection based on material removal calculation, which are mainly used to optimize the feed rate in relation to the amount of material currently being removed at a given toolpath point. These methods assume that the geometry of the input workpiece is always known for a given technological operation. The proposed method essentially involves a simplified principle in order to allow easy usability for finishing toolpaths. As seen in Fig. 2, the remaining material can be in simplification considered as an equidistant surface from the part surface. Given the fact that the toolpath tolerances are very fine during finishing operations and the toolpath points are thus very close together, it may be safely assumed that the remaining material can be simplified as the parallel plane  $\rho_1$  to the tangent plane of the part surface in the contact point as seen in Fig. 4. The  $\rho_1$  plane is parallel to the workpiece tangent plane defined in the contact point and  $\rho_1$  is offset by the height of the remaining material, resp. depth of cut ( $a_p$ ) in the direction of the workpiece normal vector. The point  $C_{pS}$  is the intersection of the plane  $\rho_1$  and workpiece normal and is given by (2). To make the solution applicable to complex workpiece shapes and any tool motion, it is necessary to take into account  $\vec{m}$  obtained as the cross product (3) of the surface normal vector and the tool motion vector given by two consecutive toolpath points  $T_{T(n)}$  and  $T_T$

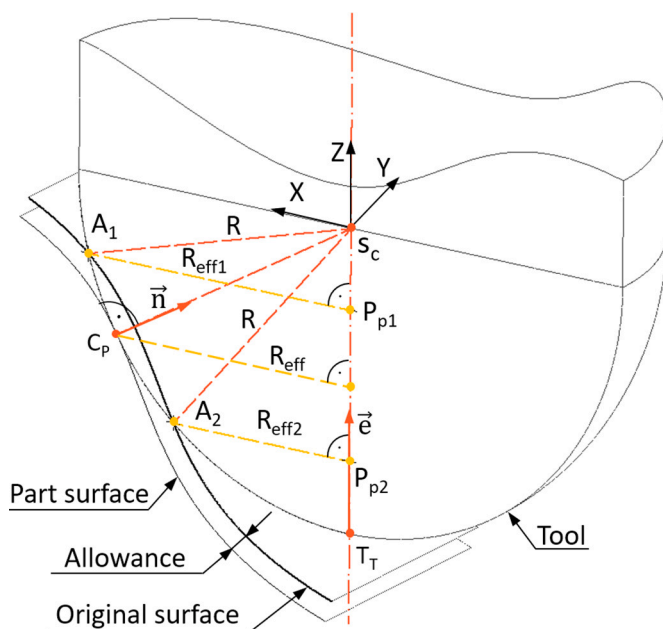


Fig. 2. Different effective cutting radii.

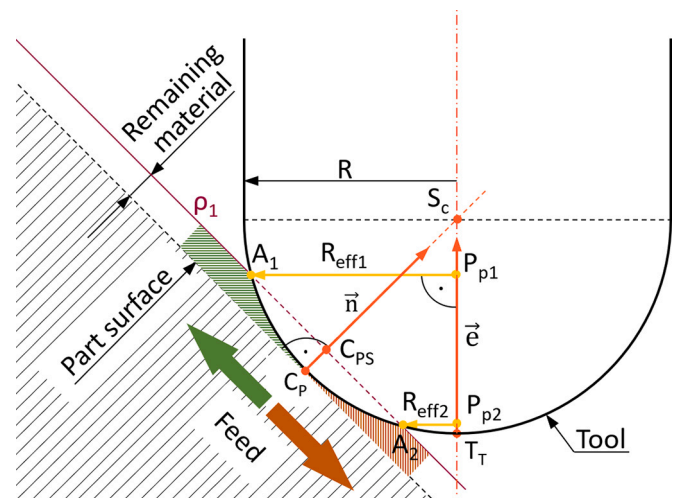


Fig. 4. Effective cutting radii given by remaining material.

(n-1). Given the fact there is still remaining material left for finishing operations, there are two intersection points, A<sub>1</sub> and A<sub>2</sub>, as seen in Fig. 4, which are used to calculate the effective cutting radius. Points A<sub>1,2</sub> are obtained by solving the set of Eqs. (4)–(8).

$$C_{PS} = C_P + \alpha p \cdot \vec{e} \tag{2}$$

$$\vec{m} = \vec{n} \times (T_{T(n)} - T_{T(n-1)}) \tag{3}$$

$$n_i \cdot A_{1,2(x)} + n_j \cdot A_{1,2(y)} + n_k \cdot A_{1,2(z)} + d_1 = 0 \tag{4}$$

$$n_i \cdot C_{P(x)} + n_j \cdot C_{PS(y)} + n_k \cdot C_{PS(z)} + d_1 = 0 \tag{5}$$

$$m_i \cdot A_{1,2(x)} + m_j \cdot A_{1,2(y)} + m_k \cdot A_{1,2(z)} + d_2 = 0 \tag{6}$$

$$m_i \cdot S_{C(x)} + m_j \cdot S_{C(y)} + m_k \cdot S_{C(z)} + d_2 = 0 \tag{7}$$

$$(A_{1,2(x)} - S_{C(x)})^2 + (A_{1,2(y)} - S_{C(y)})^2 + (A_{1,2(z)} - S_{C(z)})^2 = R^2 \tag{8}$$

The effective cutting radius is then calculated as a distance from points A<sub>1,2</sub> to the tool axis  $\vec{e}$  using formula (9).

$$R_{eff1,2} = | [S_C + |(A_{1,2} - S_C) \cdot \vec{e}| \cdot (-\vec{e}) ] - A_{1,2} | \tag{9}$$

The resulting effective cutting radius is then selected from the two variants (R<sub>eff1</sub> or R<sub>eff2</sub>) depending on which of the points, A<sub>1</sub> or A<sub>2</sub>, is located in the direction of tool movement (from the contact point).

### 3. Spindle speed acceleration and deceleration

The actual acceleration and deceleration of the spindle play an important role in determining whether or not the desired spindle speed can be achieved at particular toolpath points. If spindle acceleration and deceleration are neglected, the control system would constantly try to adjust the actual spindle speed to the desired values during the toolpath, but there would be continual jump changes that would often not even be achievable. Based on the required spindle speed, the desired feed rate must also be calculated to maintain a constant feed per tooth. Thus, as shown in previous research, the feed rate can be dynamically controlled too during the toolpath. However, the spindle acceleration and deceleration values are different for each type of spindle and its control. Therefore, if the desired spindle speed value is not achieved at particular points of the toolpath, the constant feed per tooth will not be achieved. Thus, it is essential that the calculation of the required spindle speed already includes the real possibilities of spindle acceleration and deceleration and that the required feed rate value is subsequently calculated to this value so that a constant feed per tooth is maintained. An experiment on three different machine tools (marked as A, B and C) with three different spindles was performed. Machine tool A is equipped with a spindle with gear transmission and a maximum spindle speed of 4000 RPM. Machine tool B is equipped with a spindle with direct drive and a maximum spindle speed of 15,000 RPM. Machine tool C is equipped with a spindle with direct drive and a maximum spindle speed of 40,000 RPM. Spindle speed was measured using a laser surface velocimeter. The goal was to determine whether the acceleration and deceleration have the same characteristics and identify the profile of the velocity function.

The measurement performed on machine tool B can be seen in Fig. 5. Three velocity profile characteristics were measured for the three selected spindle speed values. The characteristic comprises three sections. At first the spindle accelerates from 0 to the selected spindle speed, then the spindle speed is constant and the last section is the deceleration to 0. As seen in Fig. 5, the acceleration and deceleration form a linear function in the measured characteristic and this was the case for all three spindles (of machine tools A, B and C). Given this fact, a spindle acceleration value can be computed simply from the increment of spindle speed S and increment of time t using formula (10).

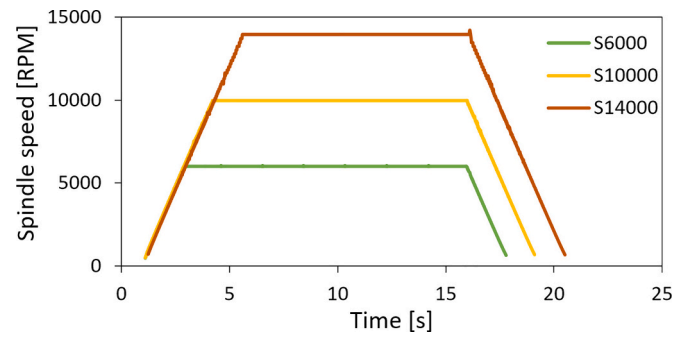


Fig. 5. Measured spindle speed characteristics (of the spindle of machine tool B).

Table 1  
Acceleration of selected spindles.

Machine tool	A	B	C
Spindle drive	Gear transmission	Direct drive	Direct drive
Max. spindle speed [RPM]	4000	15,000	40,000
Spindle acceleration [rad/s <sup>2</sup> ]	131	227	751

$$\alpha = |\Delta S|/|\Delta t| \tag{10}$$

Table 1 provides an overview of the measured acceleration values of the tested spindles. It can be clearly seen that the acceleration values for all three spindles differ significantly. This means that every spindle gives a different possibility for achieving the required spindle speed value along the toolpath when the spindle speed is controlled dynamically in each toolpath point. The goal of dynamically controlled spindle speed is to achieve a constant cutting speed. When the spindle speed is changing, the feed rate must be controlled at the same time to achieve a constant feed per tooth. As mentioned earlier, it is crucial to know the real spindle speed to control the feed per tooth. It was found that the deceleration values are set to the same value as the acceleration. Therefore, the acceleration and deceleration of the specific spindle have to be included in the calculation of the required spindle speed.

### 4. Proposal of spindle speed and feed rate control method

A new spindle speed calculation method based on knowledge of spindle kinematic parameters (acceleration and deceleration) and effective cutting radius was proposed.

#### 4.1. Algorithm for spindle speed and feed rate control including spindle kinematics

The acceleration and deceleration values are used to propose an algorithm, which calculates the required spindle speed value at each toolpath point. At first the effective cutting radius is calculated based on knowledge of an actual toolpath point, the tool axis vector and contact point between the tool and the workpiece, as well as the cutting speed and feed per tooth. These parameters are commonly known as output from the CAM system in the form of cutter location data (CL data). The required spindle speed is then calculated based on the effective cutting radius to maintain the required cutting speed. The spindle speed value and feed per tooth are then used to calculate the feed rate and subsequently the cutting time is calculated. Knowledge of acceleration and deceleration enables calculation of the real increase or decrease in spindle speed at each toolpath point to obtain the achievable spindle speed. If the required spindle speed is beyond the limit given by the achievable spindle speed, then the achievable spindle speed value must be set as the required spindle speed to calculate the final feed rate. If the required spindle speed is below the limit given by the achievable spindle

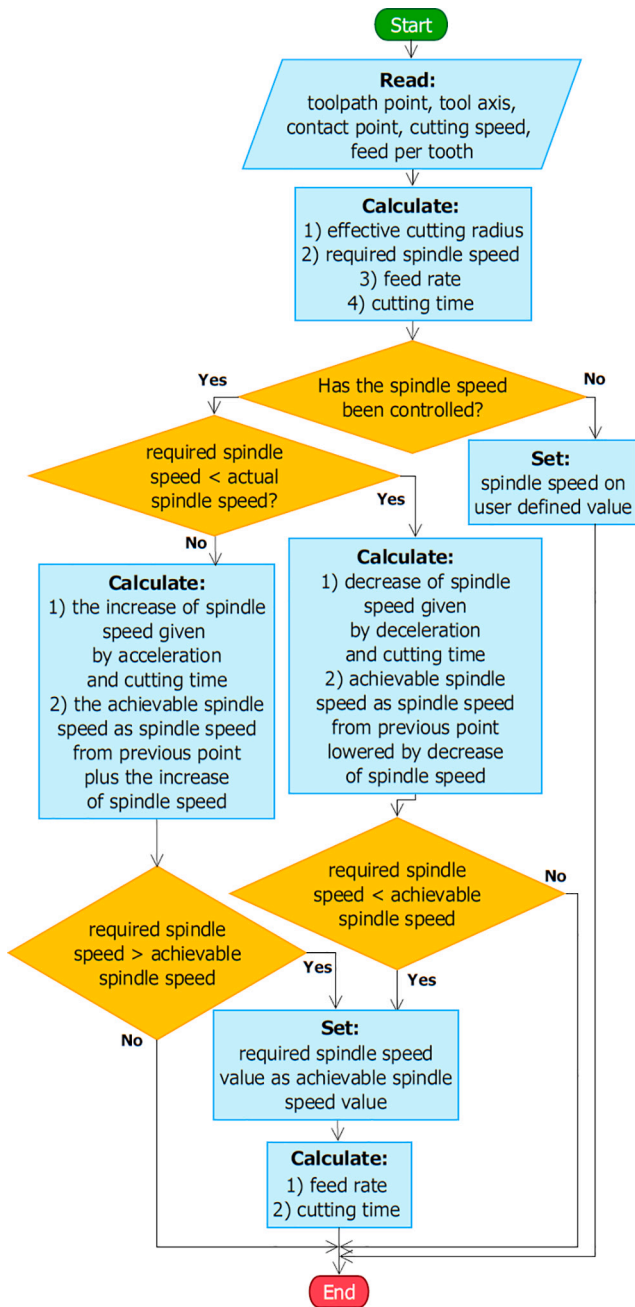


Fig. 6. Calculation of cutting conditions.

speed, then the final feed rate is calculated from the required spindle speed. This method of calculating the required spindle speed and feed rate while maintaining the constant cutting speed and feed per tooth is expressed by the flow chart in Fig. 6.

4.2. Method enhancement by spindle speed and feed rate control concerning the remaining material

As mentioned earlier, there are two methods to calculate the effective cutting radius. One approach deals only with the contact point, while the second also considers the remaining material. Both options can be used as the basis for calculation of the required spindle speed. Therefore, the proposed spindle speed and feed rate control method has been enhanced by an effective cutting radius calculation based on the remaining material. The algorithm can be seen in Fig. 7.

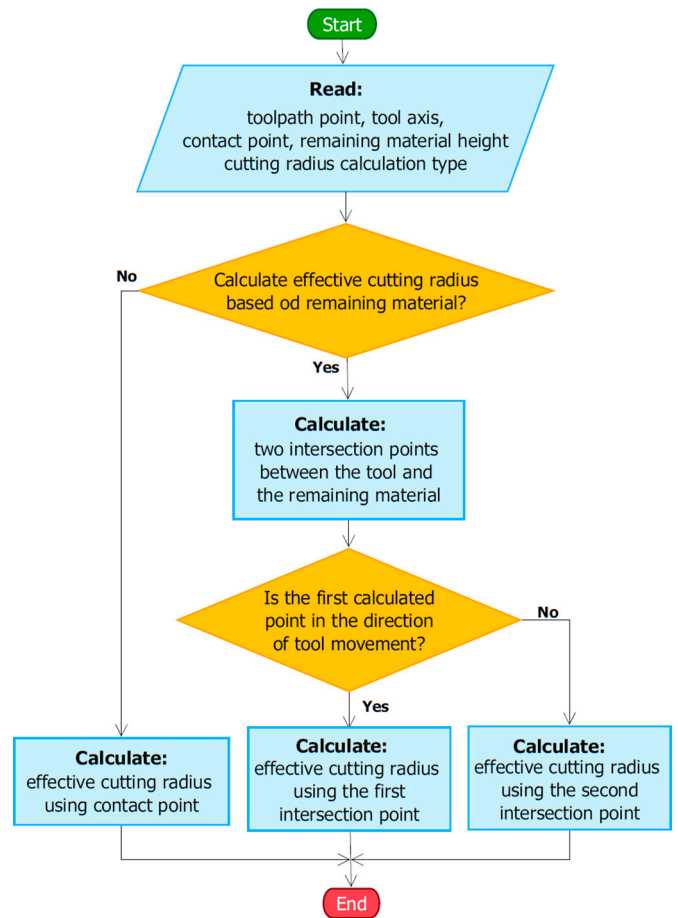


Fig. 7. Calculation of effective cutting radius.

4.3. Dynamic spindle speed and feed rate control based on the proposed method

The two proposed algorithms of the new method were tested in the form of an optimization function in the postprocessor for Siemens NX CAM. Additionally, a new functionality was implemented in the postprocessor that can generate data to verify the optimized NC programs by coloured toolpaths directly in the CAM system. This is a benefit for the technologist, who can verify and possibly rearrange the cutting conditions in regard to specific needs. The toolpaths may be coloured according to the spindle speed, feed rate or effective cutting diameter achieved at the toolpath points. This is only an additional functionality, the main functionality is the generation of optimized NC program, where the cutting conditions are automatically optimized to achieve the constant cutting speed and feed per tooth without requiring any

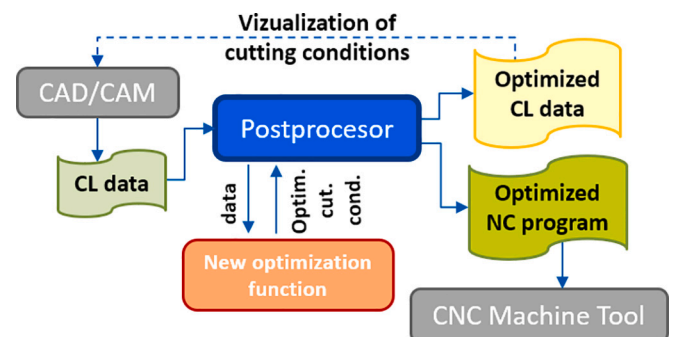


Fig. 8. Optimized NC program generation workflow.

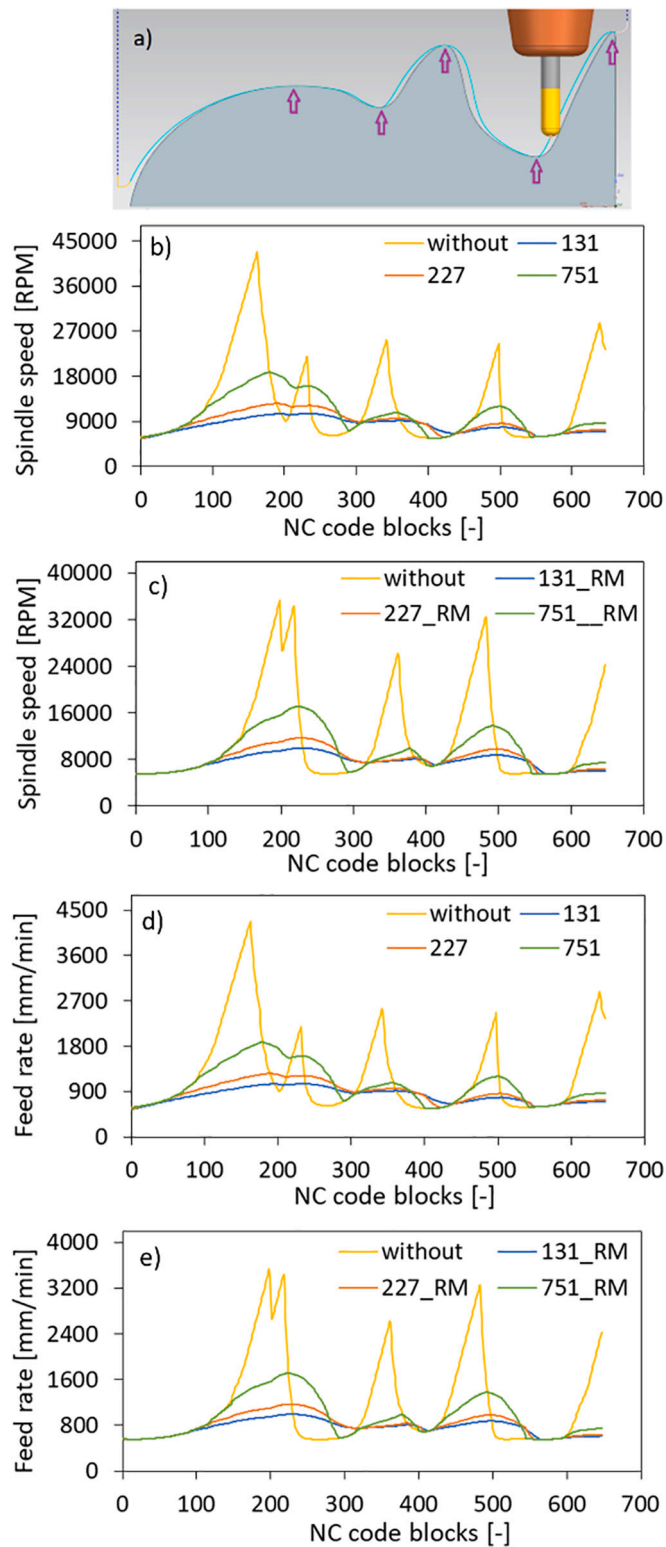


Fig. 9. Toolpath and characteristics of cutting conditions for different acceleration and deceleration values.

additional action from the technologist. This means that no toolpath modifications are needed. The workflow of optimized NC program generation can be seen in Fig. 8.

A complex shape and the toolpath (Fig. 9a) were proposed to further analyze the impact of the specific spindle acceleration and deceleration values on the spindle speed and feed rate characteristics while using the

proposed optimization method. A milling tool with the diameter of 4 mm and 2 teeth was applied for this analysis and the feed per tooth was set on the value of 0,05 mm and cutting speed was set on the value of 70 m/min.

The spindle speed and feed rate characteristics were obtained for the three different spindle acceleration values as given in Table 1 when using the optimization method, but for this analysis no maximum spindle speed limit was applied. The characteristics were compared for both ways of calculating the effective cutting radius. The characteristics are marked as follows. The characteristics for the three different spindles are differentiated and marked by indicating the acceleration value directly (e.g. 227, which corresponds to 227 rad/s<sup>-2</sup>). In addition, one more spindle speed characteristic was added, which was obtained on the basis of the old method for spindle speed calculation, i.e. without the new optimization algorithm (without acceleration and deceleration parameters of the spindle), and this characteristic is identified as “without”. The characteristics obtained on the basis of effective cutting radius calculated from the contact point do not have any additional identification marks. The workpiece with the height of the remaining material set at 0.2 mm (depth of cut) for the finishing operation and analysis of characteristics. The characteristics obtained on the basis of effective cutting radius calculated from the remaining material are identified with added “\_RM” (e.g. 227\_RM). All the characteristics are shown in Fig. 9(b-e). Significant differences can be found in the spindle speed and feed rate characteristics. The ideal spindle speed characteristic to achieve a constant cutting speed is the marked as “without” (Fig. 9b). Five peaks can be found on this characteristic, which correspond to the contact points between the workpiece and the tool, there the real cutting radius is close to zero (marked by violet arrows in Fig. 9a), i.e. near to the tool tip. The spindle speed at these points do not go to infinity, since the contact point between tool and workpiece is not calculated for points exactly on the tool tip, but only close to it. However, no spindle can achieve this characteristic because of acceleration and deceleration limits. It can be clearly seen that the higher the spindle acceleration and deceleration value, the more the algorithm is able to follow the necessary spindle speed to maintain the required cutting speed in the widest possible toolpath range (Fig. 9b and c).

At the same time, it is also clear from the feed rate characteristics that the higher the spindle acceleration and deceleration values, the higher the feed rate values achieved (Fig. 9d and e, which of course means a higher savings in machining time. By comparing the spindle speed characteristics, it is also evident that the algorithm is able to detect how the effective cutting radius changes while respecting the remaining material. When respecting the remaining material, the achieved speeds are also proportional to whether the toolpath section is downward or upward in terms of tool movement (Fig. 9c). In general, lower spindle speeds are achieved on the upward sections than on the downward sections, where higher speeds are achieved when compared to the spindle speeds when only the contact point between the tool and the workpiece is considered. This showed the effects of the newly developed optimization method in general. The last graph in this section (Fig. 10) shows the feed per tooth characteristics for the case when the ideal

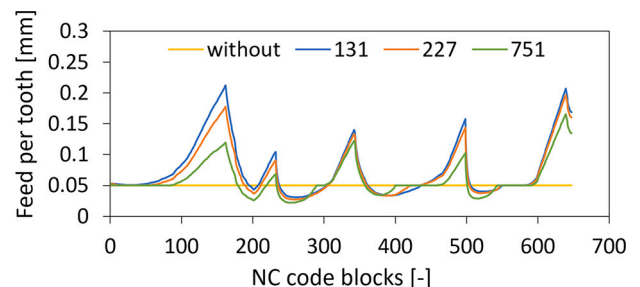


Fig. 10. Characteristics of feed per tooth for three real spindles when the new optimization is not used.

spindle speeds and feed rates are calculated using the old method, i.e. without the new optimization method. The characteristics clearly show that in the case of a real spindles with acceleration and deceleration limits, the required feed per tooth is not achieved. This occurs because the machine tool drives are able to follow the required feed rate, but in the same time the spindle does not reach the required spindle speed values, and thus the required feed per tooth is either reduced or exceeded in relation to the required feed rates. The next necessary step was to verify the effects of using the optimization method in real machining.

### 5. Experimental verification

The intention is to verify the benefits of the proposed Optimization method on tool life and machining time reduction. Therefore a bowl-shaped mould (Fig. 11) made of difficult-to-cut stainless steel 1.4462 was chosen as the testing part. Given the changing surface angle, it is convenient to demonstrate the advantages, differences, and potential of the optimization method.

#### 5.1. Spindle speed characteristics when using the optimization function

In this step, the effect of input values (tool diameter and the height of the remaining material) on the spindle speed characteristics were analysed. The differences are shown by using only one tool pass exactly in the middle of the workpiece (Fig. 12a).

Fig. 12b shows the characteristics of effective diameter calculated by contact point for three diameters of ball-end mill (6; 10; and 16 mm). The values of effective diameter are used instead of effective radius so that changes from the nominal value of the ball-end mill diameter can be seen more clearly. The characteristics of effective diameter calculated by remaining material for the same three diameters of ballend mill are shown in Fig. 12c. It can be clearly seen that effective cutting diameter is lower on the downward section of toolpath then on the upward section of the toolpath. The effect of three different heights of remaining material (0.1; 0.2 and 0.3 mm) on the effective diameter for the tool

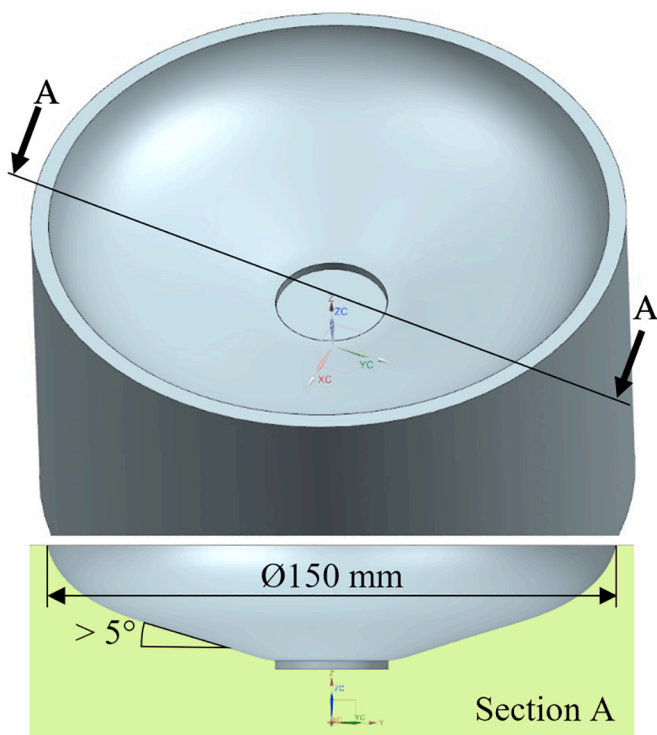


Fig. 11. Bowl shaped mould.

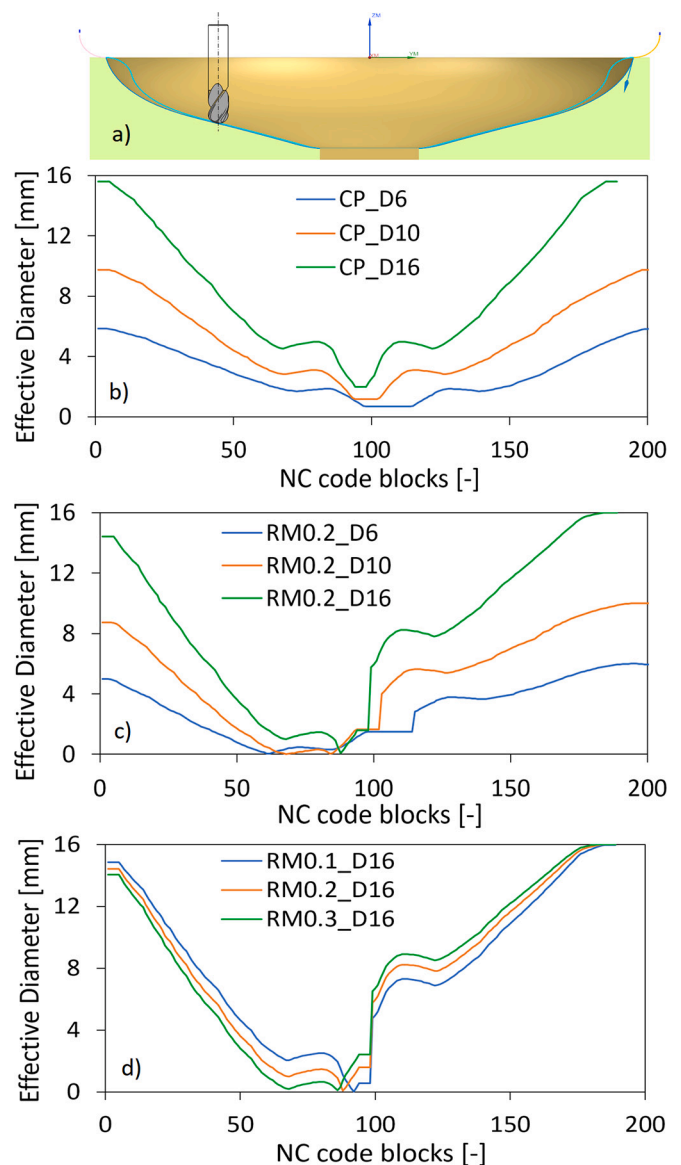


Fig. 12. Toolpath and effective diameter characteristics for different tool diameters and remaining material heights.

diameter of 16 mm is shown in Fig. 12d. On the downward section of the toolpath, the resulting effective tool diameter is smaller for higher values of the height of the remaining material due to the fact that the remaining material intersects the tool envelope closer to the tool axis than it does for lower values of the height of the remaining material. The characteristics of spindle speed and feed rate according to the calculated effective diameter values are seen in Fig. 13.

All the following characteristics in this chapter are obtained for the machine tool (spindle acceleration of  $227 \text{ rad/s}^2$ ) that will be further used for machining tests. Fig. 13a shows the characteristics of spindle speed calculated by the effective diameter on the basis of contact point for three diameters of ball-end mill (6; 10; and 16 mm). The corresponding characteristics of feed rate are then shown in Fig. 13d. It can be seen, that the characteristic of spindle speed (and feed rate too) for the ball-end mill with the diameter of 6 mm differs from the other two characteristics. This occurs because the ideal values of the required speed for the tool diameter of 6 mm are already so high that the spindle with the actual acceleration value is not able to achieve the spindle speed values in the same range as in the case of other two tools. Another finding is that the lower the tool diameter, the higher the spindle speed

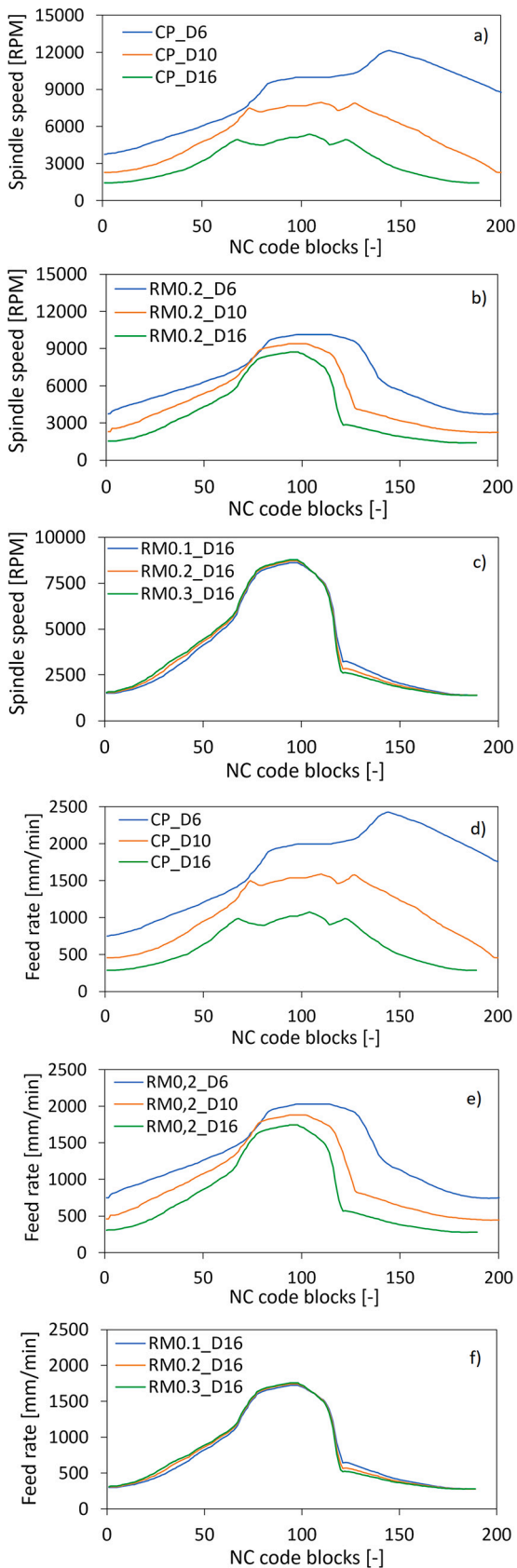


Fig. 13. Spindle speed and feed rate characteristics.

must be achieved. It was already mentioned above that the higher the achieved spindle speed, the higher the resulting feed rates and therefore, the higher the productivity. Characteristics of spindle speed based on effective diameter calculated by remaining material can be seen in Fig. 13b and the corresponding characteristics of feed rates are shown in the Fig. 13e). It is clearly seen that in the middle section of the characteristics the values steadily increase and then rapidly decrease. The section of rapid decrease is not significant in the case of characteristic for a tool diameter of 6 mm. Fig. 13c shows the effect of three different usual heights of remaining material (0.1; 0.2 and 0.3 mm) on the spindle speed characteristics for a tool diameter of 16 mm. Corresponding characteristics of feed rate are shown in the Fig. 13f. It is obvious that the height of the remaining material itself has very small effect on the achievable spindle speed and feed rate values.

### 5.2. Setup of experiment

The machining is performed with a strong emphasis on the final surface quality. A Tajmac ZPS MCFV 5050 LN 3-axis milling machine tool with Sinumerik 840D control was chosen for manufacturing. This machine tool is equipped with a spindle with a maximum spindle speed of 15,000 RPM, spindle acceleration of  $227 \text{ rad/s}^{-2}$  and ISO 40 tool interface. A solid carbide ball-end mill ROTANA R-14154 with two teeth, diameter of 16 mm, helix angle of  $40^\circ$  and with RotalH coating was used for the finishing operation. The workpiece was clamped in a three-jaw-chuck as seen in Fig. 14. The selection of initial cutting conditions was primarily driven by the tool producer based on the machinability of the material. The cutting speed was set at 70 m/min and feed per tooth was set at 0.1 mm. Flood cooling was used for this experiment. Dept of cut was set at 0.2 mm. The toolpath was created using Siemens NX CAM. The milling passes on the workpiece were parallel so that the interpolation on the path was in the X-Z plane and the stepover was realized in the Y-axis. The point milling operation was programmed bidirectionally, i.e. with a „zig-zag“ strategy. Subsequently



Fig. 14. Experimental setup on the machine tool.

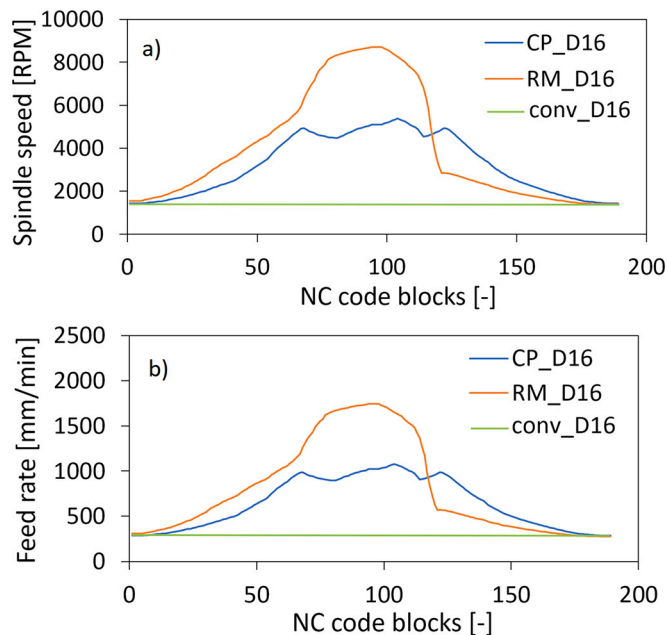


Fig. 15. Spindle speed and feed rate characteristics for three finally selected cutting operations.

the postprocessor enhanced by the new optimization function was applied to achieve the NC programs with dynamic spindle speed and feed rate control. In this case of the chosen testing part, a strategy of „spiral“ type would seem appropriate, but the „zig-zag“ strategy was chosen because it represents the most common strategy used on moulds, blades, turbines, impellers, etc.

```

N100 T04 D01
N102 G55
N104 S1428 M03
N106 G00 X73.144 Y0 Z14.679
N108 M08
N110 G01 Z3 F279
N112 Y0.0 Z-1.547
N114 X73.124 Z-1.635
N116 X72.494 Z-4.388
N118 X72.179 Z-5.766
N120 X72.022 Z-6.436 F287
N122 X71.865 Z-7.008 S1436 F291
N124 X71.55 Z-7.914 S1452 F299
N126 X71.235 Z-8.64 S1497 F308
N128 X70.92 Z-9.261 S1543 F317
N130 X70.606 Z-9.809 S1581 F326
N132 X70.306 Z-10.281 S1626 F334
N134 X70.006 Z-10.716 S1672 F343
N136 X69.406 Z-11.498 S1710 F360
N138 X68.806 Z-12.193 S1801 F377
N140 X68.206 Z-12.821 S1885 F394
N142 X67.606 Z-13.397 S1968 F411
N144 X67.006 Z-13.93 S2052 F428
N146 X66.406 Z-14.428 S2136 F445

```

Fig. 16. Example of initial section of NC program with spindle speed and feed rate control.

The final comparison between spindle speed characteristics given by the two optimization functions based on different calculation of effective cutting radius that will be used for machining tests can be seen in Fig. 15a. The conventional NC program has a constant spindle speed and this is shown by the green line (label conv\_D16) in Fig. 15a as well. Both optimization functions increase the spindle speed to maintain the constant cutting speed. The characteristics of spindle speed calculated by the method that uses the contact point are marked in blue (label CP\_D16) and the characteristics of spindle speed calculated by the approach that uses the remaining material are marked in orange (label RM\_D16). Corresponding feed rate characteristics are shown in Fig. 15b. Different machining times are assumed as there are three different feed rates characteristics for the same toolpath. An example of NC program initial section with the changes of spindle speed and feed rate values in the NC program blocks can be seen in Fig. 16. The toolpath increment (the distance between two points in the NC blocks) varies from approx. 0.5 mm to 1 mm depending on the current surface curvature and the toolpath tolerance set in the CAM system.

Coloured toolpaths (using optimized CL data) can be seen in Fig. 17. The left side of Fig. 17 shows the characteristics of effective cutting diameter calculated on the basis of the contact point. The right side of Fig. 17 shows the characteristics of effective cutting diameter calculated on the basis of the remaining material.

## 6. Results and discussion

First, the workpiece was roughened so that finishing operations could be performed. The finishing operations were repetitions created by shifting the Z-axis by the height of the remaining material (0.2 mm). After each shape was milled (as a layer) on the workpiece, the tool was removed from the spindle and inserted with the tool holder into the fixture on the Keyence VHX-7000 microscope, where the wear on both cutting edges was measured.

### 6.1. Tool life measurement

The maximum cutting edge wear on flank, noted as  $VB_{max}$ , was evaluated. The new cutting edge compared to the cutting edge at the end of tool life is shown in Fig. 18. The machining was repeated until the wear value  $VB_{max}$  on one of the tool blades reached 200  $\mu\text{m}$ . Conventional machining of one layer took 53 min, while spindle speed and feed rate optimization based on the contact point led to a one-layer machining time of 26 min, and spindle speed and feed rate optimization based on the remaining material led to a one-layer machining time of 36 min. This means that contact point optimization more than doubled machining productivity compared to conventional milling. The machining times are shown in Table 2, along with the productivity increase. Thus, the tool life of each tool was tested up to a comparable  $VB_{max}$  limit of 200  $\mu\text{m}$ . The tool life test was performed for all three options of controlling the cutting conditions and two repetitions with new tools were performed for each option. The two wear measurements were averaged at each step (number of machined layers).

To obtain a relevant assessment of the tool life results, the machined area was calculated, since each of the three machining options had a different machining time per layer. One machined layer has an area of 2.34  $\text{dm}^2$ .

Fig. 19 shows an example of a tool cutting edge wear comparison after milling the same area, specifically after machining of eight layers (or shapes), i.e. 18.72  $\text{dm}^2$ , each by one specific tool. The wear shows that the tool that had been milling using the conventional NC program is approaching the end of its life, while the tool edges of both tools that had been milling using optimized NC programs do not show much wear. The cutting edge wear is most noticeable at the diameter that corresponds to the largest area of the toolpath, which is located on a section of the machined surface with an inclination of approximately  $5^\circ$ . The graph in Fig. 20 shows all the measured wear characteristics in relation to the

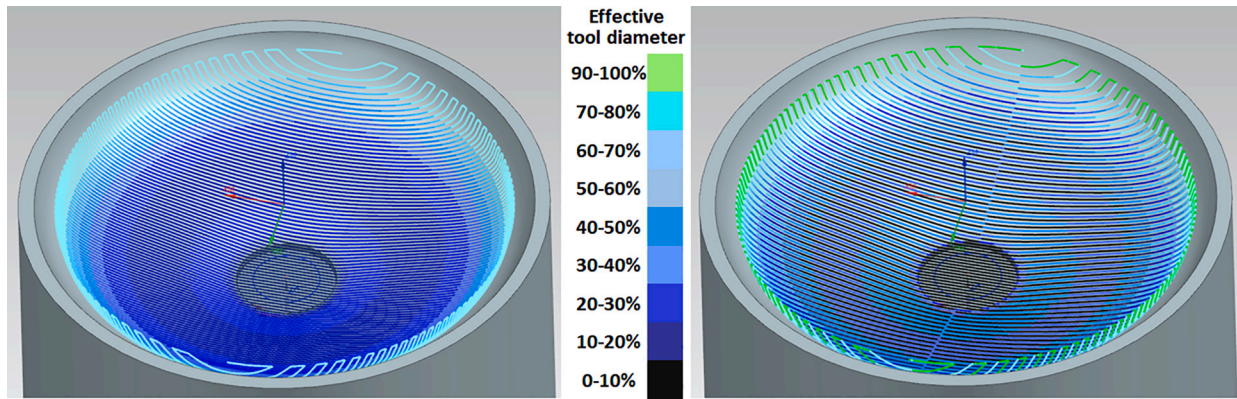


Fig. 17. Characteristics of effective cutting diameter using the coloured toolpaths (left: based on the contact point, right: based on the remaining material).

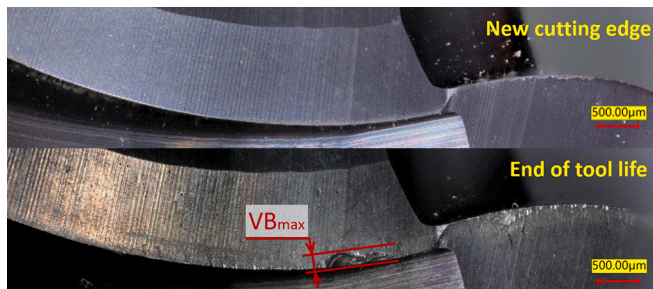


Fig. 18. Cutting edge comparison (top: new cutting edge, bottom: end of tool life).

Table 2  
Machining test results.

Tool life test	Conventional	Optimization CP	Optimization RM
Machining time per one surface [min]:	53	26	25
Number of surfaces machined per tool life [-]:	9	23.5	15.5
Total machining time (per tool life) [min]:	477	611	387.5
Total machined area (per tool life) [dm <sup>2</sup> ]:	21.06	54.99	36.27
Machining performance [dm <sup>2</sup> /h]:	2.65	5.4	5.6
Tool life change [%]:	0	+28	-19
Machining time reduction [%]:	0	51	53
Machining performance increase [%]:	0	104	111

machined area (two measurements for each conditions control type). The comparison shows that contact point optimization produces the best results in terms of the total machined area per tool life. The values from both measurements were averaged. After nine machined layers, the wear limit was reached for the tool machined under conventional speed and feed rate control, resulting in a total machined area of 21.06 dm<sup>2</sup> in a total of 477 min. Twenty-three and a half layers were machined when the tool was machined using contact point optimization, resulting in a total machined area of 54.99 dm<sup>2</sup> in a total of 611 min. The tool machined using remaining material optimization managed to machine 15.5 layers, a total of 36.27 dm<sup>2</sup> in a total of 387.5 min. These values are summarized in Table 2.

Based on the total machining times, it is evident that tool life was increased by 28 % using contact point optimization compared to

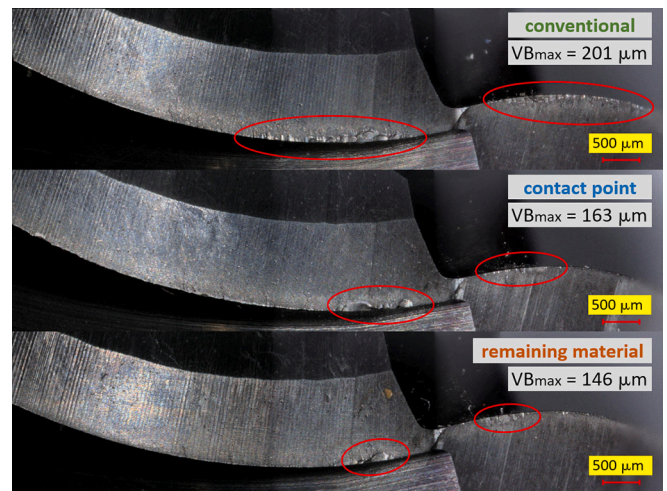


Fig. 19. Comparison of cutting edges of three machining options (after 8 machined layers).

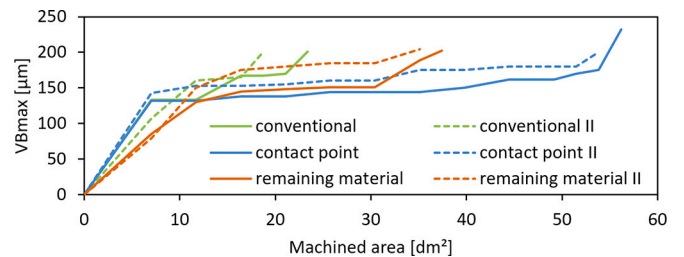


Fig. 20. Maximum tool wear on flank in relation to machined Area.

conventional machining, while tool life was decreased by 19 % using remaining material optimization compared to conventional machining. It can be clearly seen that the machining time was reduced significantly (approx. by 50 %) using both optimization methods. However, the most conclusive parameter for evaluation is machining performance, obtained as the ratio of machined area per time. The highest performance was obtained for contact point optimization. Specifically, the performance at the specified wear limit is by 104 % higher than for the conventional option. The machining performance using remaining material optimization is by 111 % higher compared to the conventional option. The machining performance values are shown in Table 2, along with the machining performance increase. Based on the evaluation, the method of optimizing the cutting conditions based on the contact point can be classified as the best option.

### 6.2. Surface roughness measurement

In order to compare the three machining options, the roughness of the machined surface was measured as well. The milling was carried out so that the toolpaths were adjusted to face the centre of the part. This made it possible to machine one layer of the part divided into three segments so that roughness could be measured and directly compared on one machined layer. The division of the surface into three segments is shown in Fig. 21. The locations from which the three detailed photographs were taken are marked in Fig. 21 for visual comparison of the surface quality achieved. A comparison of these three details is shown in Fig. 22. Through close observation of the surface machined using the conventional cutting conditions control approach (no dynamic spindle speed and feed rate control), it was clearly seen that there were areas on the machined surface where material was being stripped. These areas can be seen as scratches or stripes in Fig. 22, left. This mainly affects the even texture of the surface; they are not deep scratches. This effect was not very noticeable on the surface machined under remaining material optimization of spindle speed and feed rate control (Fig. 22, right). On the surface machined under contact point optimization of cutting conditions, these spots occurred only sporadically (Fig. 22, middle).

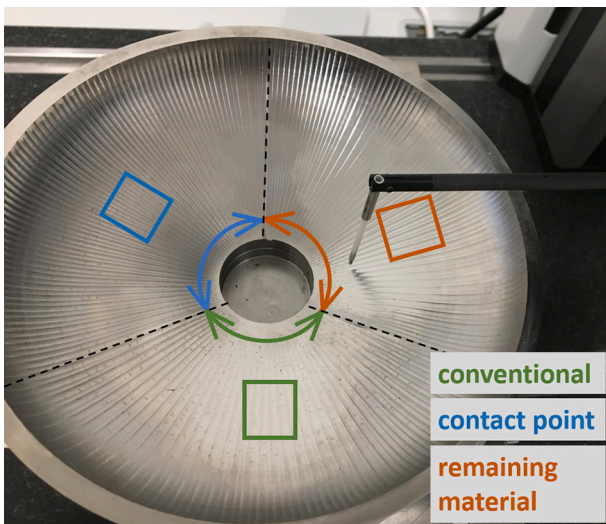


Fig. 21. Workpiece for roughness measurement.

**Table 3**  
Roughness measurement results.

Machining	Rz [ $\mu\text{m}$ ]	Ra [ $\mu\text{m}$ ]	Rsm [ $\mu\text{m}$ ]
Conventional	$1.81 \pm 0.2$	$0.30 \pm 0.03$	$59.7 \pm 19$
OPT CP	$1.92 \pm 0.46$	$0.29 \pm 0.06$	$50 \pm 17$
OPTRM	$1.86 \pm 0.32$	$0.29 \pm 0.05$	$46.9 \pm 12$

Surface roughness measurements were carried out in the direction of tool movement (along the tool path – longitudinal roughness) at four different locations on the machined surface for each of the three parts of the surface machined under different cutting conditions control options. The roughness measurements were carried out using a Mahr LD130. The averaged values from the four sets of measurements taken are shown in Table 3. It is evident that the resulting surface roughness is practically the same for all three cutting conditions control approaches. The Ra value does not exceed  $0.3 \mu\text{m}$ , which is quite satisfactory for finishing milling technology. The highest difference can be seen in the Rsm value, which shows the mean value of the distance of the grooves in the material. This value confirmed the visual observation, i.e. the influence of scratches on the machined surface topography.

### 6.3. Spindle speed and feed rate measurement

Another important verification is, whether the desired feed per tooth along the tool path was actually achieved as assumed in the optimization function, or not. For this purpose, a short toolpath of approximately two and a half passes was created, as shown in Fig. 23, and then NC programs were generated to measure the actual spindle speed and feed rate achieved in the control system. The toolpath used for the measurements is again oriented such that the interpolation during cut motion is

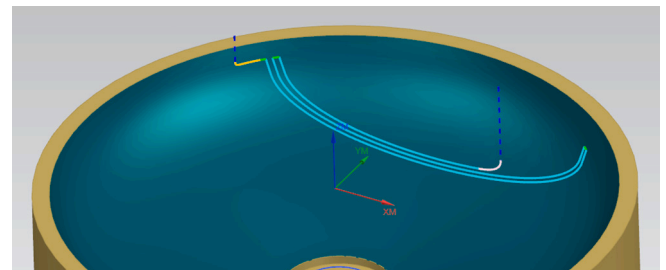


Fig. 23. Sample toolpath for measurement.



Fig. 22. Detailed comparison of surfaces (machined by three approaches).

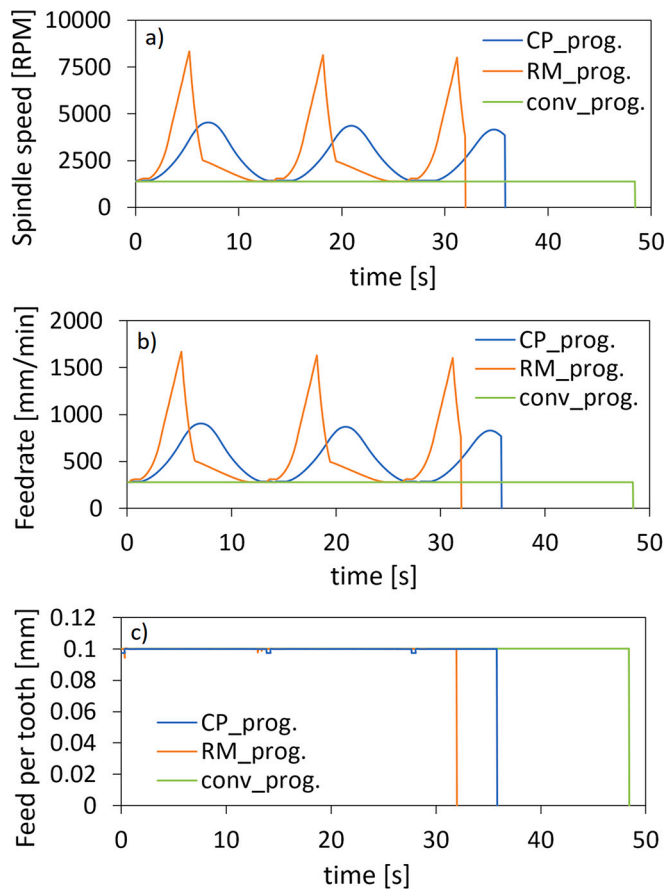


Fig. 24. Characteristics of spindle speed (a), feed rate (b) and feed per tooth (c) obtained from NC program.

performed in the X-Z plane and the Y-axis is only involved within the transition movements.

The characteristics of spindle speed obtained from the NC program can be seen in Fig. 24a and corresponding feed rate characteristics are shown in Fig. 24b. The graph in Fig. 24c proves that the planned spindle speeds and feed rates ensure a constant feed per tooth. The actual spindle speeds and feed rates achieved on machine tool were measured using servo trace function of computer numerical control.

The measured spindle speed characteristics are shown in Fig. 25a and feed rate characteristics in Fig. 25b. It can be seen that there are smooth changes in spindle speeds and feed rates when optimizing through contact point calculation of the effective cutting radius (CP\_meas.). The characteristic of real feed per tooth are seen in Fig. 25c. It is obvious that the constant feed per tooth was achieved using the optimization based on the contact point. The characteristics of spindle speed and feed rate obtained of the optimization method based on the remaining material (RM\_meas.) consist of sections with rapid increase and rapid decrease of values. It is evident from the feed per tooth characteristic that the required value of 0.1 mm is not maintained at five sections of the tool-path. These sections are marked by the Roman numerals (I., II., III., IV. and V.). Three of these sections (marked by I., III. and V.) show the decrease of feed per tooth by approx. 0.02 mm and these are the sections, where the spindle speed and feed rate are decreasing. The decrease in feed per tooth means that the feed rate decreased faster than the spindle speed. Other two sections (marked by II. and IV.) show the increase of feed per tooth by approx. 0.01 mm and these are the sections where the spindle speed and feed rate are increasing. The increase in feed per tooth means, that the feed rate increased faster, than the spindle speed. This variation in feed per tooth can also be the cause of lower tool life when using optimization using the effective radius based on

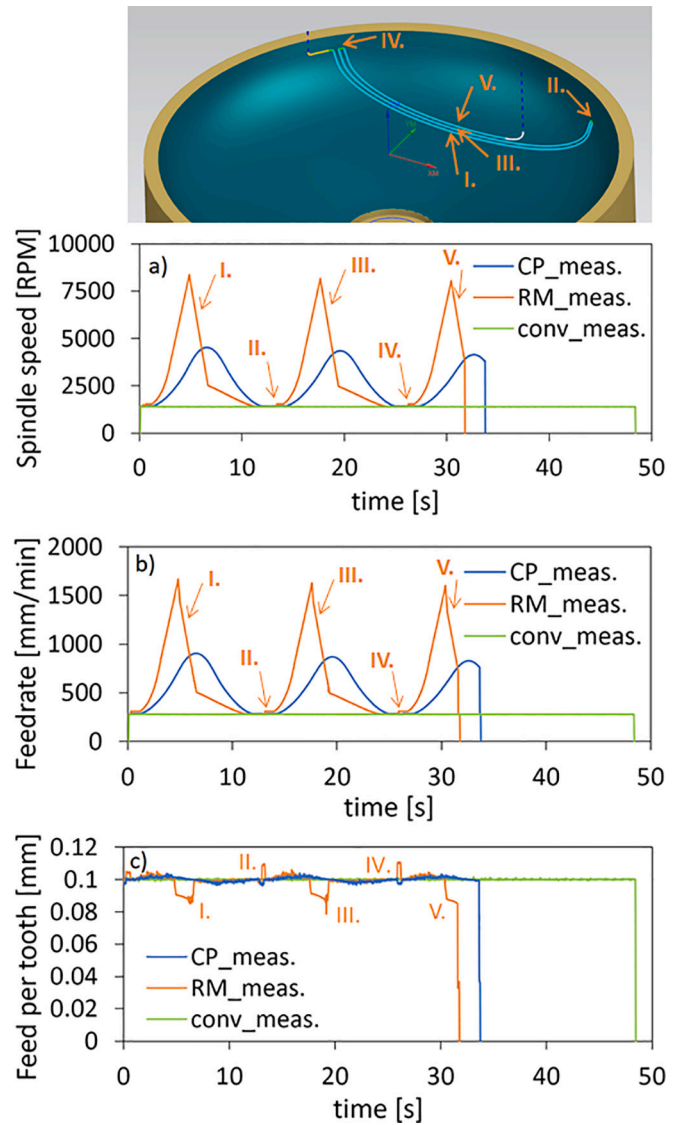


Fig. 25. Characteristics of spindle speed (a), feed rate (b) and feed per tooth (c) obtained from measurement on machine Tool.

remaining material. In addition the spindle speed and feed rate characteristics under conventional control of the cutting conditions (conv\_meas.) are shown as well. It can be concluded that the optimization works very well when using the contact point method, which was also confirmed by the machining tests. In this method, there is no risk of rapid jumps in spindle speed and feed rate control, as the changes in the tool contact point (and also the real cutting diameter) are uniform and smooth. The method of optimization using remaining material gives a sections, where the cutting conditions changes rapidly and therefore it is not appropriate for spindle speed and feed rate control.

#### 6.4. Energy consumption measurement

The energy consumption of all machine axes and spindle was measured using a Qualistar plus C.A. 8335 three-phase power analyzer. In the conventional control method, an average spindle current of 1.18 A was measured and the total energy consumption was 1128 Wh. Whereas in the case of the dynamic spindle speed and feed rate control with contact point optimization option an average current of 1.41 A was measured and the total energy consumption was only 630 Wh. This means that the energy consumption was reduced by 44 %. In the case of the dynamic spindle speed and feed rate control with remaining material

optimization option an average current of 1.43 A was measured, the total energy consumption was only 608 Wh. It is evident that the use of the cutting conditions optimization control methods is of great importance, even for the purpose of reducing the energy consumption of machining.

### 6.5. Discussion of results

Several positive effects were achieved using the proposed function for spindle speed and feed rate control aiming to maintain a constant cutting speed and feed per tooth respecting the acceleration and deceleration of spindle. In particular, an increase in tool life of about 28 %, a reduction of machining time of about 51 % and an increase in machining performance of 104 % were achieved when optimization based on the contact point was used. It was also confirmed that there was absolutely no degradation in the roughness of the machined surface. Thanks to the proposed function that considers spindle acceleration and deceleration during spindle speed control due to the change in the effective cutting radius, the real achievable spindle speed is calculated and it is possible to recalculate the feed rate to maintain a constant feed per tooth. These benefits are incredibly high, with no degradation in any particular monitored parameter. The only parameter that “degrades” under spindle speed control is the average spindle current. This happens because the dynamic spindle speed control has actually made the spindle an additional controlled axis. However, the total energy consumption during machining is lower, mainly due to the reduction in machining time. It is also clear that this method of controlling process conditions is not suitable for all types of spindle units. For example, for machine tools that have spindle units with a drive comprising a motor and gears, this spindle speed control method will not be suitable as the spindle acceleration will be very low and the maximum spindle speed on these types of spindles is not high (typically about 3500 RPM). This function is most useful on direct drive spindles with high acceleration values. The spindle acceleration value can often be adjusted in conjunction with the manufacturer or machine tool provider, but we do not necessarily recommend setting the highest acceleration values, as this leads to an increase in the peak current flowing through the controller. In this paper it has been shown that even a spindle acceleration of  $227 \text{ rad/s}^{-2}$  is perfectly sufficient to reap the high benefits of this optimization function, even though it is not the highest spindle acceleration value. It has been found that today's spindle controllers also allow, for example, an acceleration of  $751 \text{ rad/s}^{-2}$  (see above). However, such an acceleration value is particularly suitable for cases where the spindle must be able to achieve the desired speed in the shortest possible time, which occurs for example during tool changes, thus for processes with frequent tool changes, maximum acceleration values are necessary to achieve the most productive machining times. Since spindle controllers are not yet equipped like motion axis controllers with various functions to smooth out the controlled values, such as lookahead, etc., it is preferable to avoid overloading the controller with shock changes and therefore it is certainly better not to select high acceleration values. Furthermore, it can be stated that the optimization function is most useful in machining materials that do not require high cutting speeds, e.g. steel or stainless steel, but especially difficult-to-cut materials such as duplex steel, nickel alloys, etc. On the other hand, this function is of least use for materials requiring high cutting speeds, such as various aluminium alloys, etc., where high spindle speeds will be required, particularly around the tip of the ball mill where the effective cutting diameter is small. The aim of the paper was to contribute to the deepening of knowledge in the only partially explored issue of determining the effective cutting diameter of the tool when milling shaped surfaces as well. Two methods were established for calculating the effective cutting radius of the tool: one that works with the contact point between the tool and the workpiece and the other that works with the height of the remaining material. Both methods were compared to conventional cutting conditions control. Higher benefits in all performance parameters were shown from the

cutting conditions control method in which the effective tool diameter is calculated based on the contact point between the tool and the workpiece. On the other hand, the cutting conditions control method in which the effective cutting radius of the tool is calculated based on remaining material showed slightly better results during visual inspection of the machined surface quality, but the difference was not very large. A very different results were obtained when assessing the tool life based on the total machining time, where the optimization based on the remaining material showed a worse result than the conventional control of the cutting conditions. Although the test demonstrated higher benefits from the first effective cutting radius calculation method, it was not possible to carry out a sufficient number of tests to compare these methods effectively enough, especially for different diameters of ball-end mills. It is important to add that this cutting conditions control technique can be applied not only to finishing but also to semi-finishing operations. Therefore, both cutting radius calculation methods are presented so that the technologist can investigate both cases for specific machining case, i.e. taking into account the given part and tool geometry, and then select the most suitable option. As mentioned, the specific geometry of the part surface, maximum spindle speed, acceleration of the spindle and tool radius has a large influence on the specific potential of this function.

## 7. Conclusion

A new method of spindle speed and feed rate control for point milling of complex shaped surfaces was proposed to maintain the constant cutting speed as well as the feed per tooth. This new method is based on the implementation of real spindle control parameters. Therefore, spindle acceleration and deceleration are taken into account to automatically calculate the required spindle speed and feed rate into the NC program. The new method is prepared for 3-axis as so as for multi-axis milling. An alternative method of calculating the effective tool cutting diameter for the dynamic speed and feed rate control method with respect to remaining material was proposed. An increase of tool life by 28 %, increase of productivity by 51 % and finally an increase of tool performance by 104 % when milling a part made of difficult-to-cut material (duplex steel) using dynamic spindle speed and feed rate control were achieved. It has been verified that the newly developed method improves the cutting process by maintaining a constant cutting speed and feed per tooth and the benefits mentioned above are significant. The new method was implemented into the postprocessor, which means that it can be used for automatic generation of NC programs from the CAM system without requiring any additional action from the technologist. This new function can be implemented into the CAM system directly as well.

### CRedit authorship contribution statement

**Petr Vavruska:** Conceptualization, Methodology, Visualization, Writing – original draft. **Filip Bartos:** Software, Data curation. **Michal Stejskal:** Methodology, Data curation, Formal analysis. **Matej Pesice:** Investigation, Data curation. **Pavel Zeman:** Project administration, Funding acquisition, Validation. **Petr Heinrich:** Writing – review & editing.

### Declaration of competing interest

The authors declare the following financial interests/personal relationships which may be considered as potential competing interests: Pavel Zeman reports financial support was provided by Ministry of Education Youth and Sports of the Czech Republic. Petr Vavruska reports a relationship with Czech Technical University in Prague Faculty of Mechanical Engineering that includes: employment. Petr Vavruska has patent A method of speed and feed control of machine tools and a device for performing this method issued to Czech Technical University in

Prague, Faculty of Mechanical Engineering, Department of Production Machines and Equipment.

## Acknowledgements

The authors would like to acknowledge funding support from the Czech Ministry of Education, Youth and Sports under the project CZ.02.1.01/0.0/0.0/16\_026/0008404 “Machine Tools and Precision Engineering” financed by the OP RDE (ERDF). The project is also co-financed by the European Union. The work of one of the authors was also supported by the Grant Agency of the Czech Technical University in Prague, grant no. SGS22/159/OHK2/3T/12.

## References

- [1] Batista MF, Rodrigues AR, Coelho RT. Modelling and characterisation of roughness of moulds produced by high-speed machining with ball-nose end mill. *J Eng Manuf. Proc IMechE Part B* 2015;1–12. <https://doi.org/10.1177/0954405415584898>.
- [2] Kroft L, Hnátk J, Bíčová K. Influence of tool diameter on quality of completed radio area. In: Proc 30th Int DAAAM Symp “Intelligent Manufacturing & Automation” 30; 2019. <https://doi.org/10.2507/30th.daaam.proceedings.076>.
- [3] Ozturk E, Tunc LT, Budak E. Investigation of lead and tilt angle effects in 5-axis ball-end milling processes. *Int J Mach Tool Manuf* 2009;49:1053–62. <https://doi.org/10.1016/j.ijmactools.2009.07.013>.
- [4] Wojciechowski S, Twardowski P, Wiecezowski M. Surface texture analysis after ball end milling with various surface inclination of hardened steel. *Metrol Meas Syst* 2014;1:145–56. <https://doi.org/10.2478/mms-2014-0014>.
- [5] Aspinwall DK, Dewes RC, Ng E-G, Sage C, Soo SL. The influence of cutter orientation and workpiece angle on machinability when high-speed milling inconel 718 under finishing conditions. *Int J Mach Tool Manuf* 2007;47:1839–46. <https://doi.org/10.1016/j.ijmactools.2007.04.007>.
- [6] Feng H-Y, Su N. Integrated tool path and feed rate optimization for the finishing machining of 3D plane surfaces. *Int J Mach Tool Manuf* 2000;40:1557–72. [https://doi.org/10.1016/S0890-6955\(00\)00025-0](https://doi.org/10.1016/S0890-6955(00)00025-0).
- [7] Xu G, Chen J, Zhou H, Yang J, Hu P, Dai W. Multi-objective feedrate optimization method of end milling using the internal data of the CNC system. *Int J Adv Manuf Technol* 2019;101:715–31. <https://doi.org/10.1007/s00170-018-2923-8>.
- [8] Rattunde L, Laptev I, Klenske ED, Möhring HCh. Safe optimization for feedrate scheduling of power-constrained milling processes by using Gaussian processes. *Proc CIRP* 2021;99:127–32. <https://doi.org/10.1016/j.procir.2021.03.020>.
- [9] Tounsi N, Elbustawi MA. Enhancement of productivity by intelligent programming of feed rate in 3-axis milling. *Mach Sci Technol* 2001;5:393–414. <https://doi.org/10.1081/MST-100108622>.
- [10] Salami R, Sadeghi MH, Motakef B. Feed rate optimization for 3-axis ball-end milling of sculptured surfaces. *Int J Mach Tool Manuf* 2007;47:760–7. <https://doi.org/10.1016/j.ijmactools.2006.09.011>.
- [11] Erkorkmaz K, Layegh SE, Lazoglu I, Erdim H. Feedrate optimization for freeform milling considering constraints from the feed drive system and process mechanics. *CIRP Ann Manuf Technol* 2013;62:395–8. <https://doi.org/10.1016/j.cirp.2013.03.084>.
- [12] Wei ZC, Wang MJ, Zhu JN, Gu LY. Cutting force prediction in ball end milling of sculptured surface with Z-level contouring tool path. *Int J Mach Tool Manuf* 2011;51:428–32. <https://doi.org/10.1016/j.ijmactools.2011.01.011>.
- [13] Merdol SD, Altintas Y. Virtual cutting and optimization of three-axis milling processes. *Int J Mach Tool Manuf* 2008;48:1063–71. <https://doi.org/10.1016/j.ijmactools.2008.03.004>.
- [14] Al-Regib E, Ni J, Lee SH. Programming spindle speed variation for machine tool chatter suppression. *Int J Mach Tool Manuf* 2003;43:1229–40. [https://doi.org/10.1016/S0890-6955\(03\)00126-3](https://doi.org/10.1016/S0890-6955(03)00126-3).
- [15] Yamato S, Ito T, Matsuzaki H, Fujita J, Kakinuma Y. Self-acting optimal design of spindle speed variation for regenerative chatter suppression based on novel analysis of internal process energy behavior. *Int J Mach Tool Manuf* 2020;159:103639. <https://doi.org/10.1016/j.ijmactools.2020.103639>.
- [16] Albertelli P, Mussi V, Monno M. The analysis of tool life and wear mechanisms in spindle speed variation machining. *Int J Adv Manuf Technol* 2014;72:1051–61. <https://doi.org/10.1007/s00170-014-5736-4>.
- [17] Kroft L, Hnátk J, Bíčová K. The effect of the strategy of finishing on dimensional accuracy. In: Proc 28th Int DAAAM symposium “intelligent manufacturing & automation” 28; 2017. <https://doi.org/10.2507/28th.daaam.proceedings.081>.
- [18] Vavruska P, Zeman P, Stejskal M. Reducing machining time by pre-process control of spindle speed and feed-rate in milling strategies. *Proc CIRP* 2018;77:578–81. <https://doi.org/10.1016/j.procir.2018.08.216>.
- [19] Stejskal M, Vavruska P, Zeman P, Lomicka J. Optimization of tool Axis orientations in multi-Axis toolpaths to increase surface quality and productivity. *Proc CIRP* 2021;101:69–72. <https://doi.org/10.1016/j.procir.2021.03.124>.
- [20] Berthold J, Kolouch M, Regel J, Putz M. Investigation of the dynamic behavior of machine tools during cutting by operational modal analysis. *MM Sci J* 2019. [https://doi.org/10.17973/MMSJ.2019\\_11\\_2019054](https://doi.org/10.17973/MMSJ.2019_11_2019054). Special Issue, 030.
- [21] Seguy S, Insperger T, Arnaud L, Desein G, Peigné G. On the stability of high-speed milling with spindle speed variation. *Int J Adv Manuf Technol* 2010;48:883–95. <https://doi.org/10.1007/s00170-009-2336-9>.
- [22] Käsemöller RB, de Souza AF, Voigt R, Basso I, Rodrigues AR. CAD/CAM interfaced algorithm reduces cutting force, roughness, and machining time in free-form milling. *Int J Adv Manuf Technol* 2020;107:1883–900. <https://doi.org/10.1007/s00170-020-05143-x>.
- [23] Vavruska P, Sulitka M, Stejskal M, Šimůnek A, Falta J, Heinrich P, Kopal M. Machining of thin blade using vibration prediction and continuous spindle speed control. *MM Sci J* 2019. [https://doi.org/10.17973/MMSJ.2019\\_11\\_2019089](https://doi.org/10.17973/MMSJ.2019_11_2019089). Special Issue, 119.
- [24] Maslo S, Menezes B, Kienast P, Ganser P, Bergs T. Improving dynamic process stability in milling of thin-walled workpieces by optimization of spindle speed based on a linear parameter-varying model. *Proc CIRP* 2020;93:850–5. <https://doi.org/10.1016/j.procir.2020.03.092>.
- [25] Munoa J, Bedaert X, Dombvari Z, Altintas Y, Budak E, Brecher C, Stepan G. Chatter suppression techniques in metal cutting. *CIRP Ann* 2016;65:785–808. <https://doi.org/10.1016/j.cirp.2016.06.004>.
- [26] Kalinski KJ, Galewski MA. Optimal spindle speed determination for vibration reduction during ball-end milling of flexible details. *Int J Mach Tool Manuf* 2015;92:19–30. <https://doi.org/10.1016/j.ijmactools.2015.02.008>.
- [27] Bediaga I, Munoa J, Hernández J, López de Lacalle LN. An automatic spindle speed selection strategy to obtain stability in high-speed milling. *Int J Mach Tools Manuf* 2009;49:384–94. <https://doi.org/10.1016/j.ijmactools.2008.12.003>.
- [28] Fan J. Cutting speed modelling in ball nose milling applications. *Int J Adv Manuf Technol* 2014;73:161–71. <https://doi.org/10.1007/s00170-014-5672-3>.
- [29] de Souza AF, Diniz AE, Rodrigues AR, Coelho RT. Investigating the cutting phenomena in free-form milling using a ball-end cutting tool for die and mould manufacturing. *Int J Adv Manuf Technol* 2014;71:1565–77. <https://doi.org/10.1007/s00170-013-5579-4>.
- [30] Tuysuz O, Altintas Y, Feng HY. Prediction of cutting forces in three and five-axis ball-end milling with tool indentation effect. *Int J Mach Tool Manuf* 2013;66:66–81. <https://doi.org/10.1016/j.ijmactools.2012.12.002>.
- [31] Scandiffio I, Diniz AE, de Souza AF. Evaluating surface roughness, tool life, and machining force when milling free-form shapes on hardened AISI D6 steel. *Int J Adv Manuf Technol* 2016;82:2075–86. <https://doi.org/10.1007/s00170-015-7525-0>.
- [32] Wojciechowski S. The estimation of cutting forces and specific force coefficients during finishing ball end milling of inclined surfaces. *Int J Mach Tool Manuf* 2015;89:110–23. <https://doi.org/10.1016/j.ijmactools.2014.10.006>.
- [33] Sun G, Wright P. Simulation-based cutting parameter selection for ball end milling. *J Manuf Syst* 2005;24:352–65. [https://doi.org/10.1016/S0278-6125\(05\)80019-6](https://doi.org/10.1016/S0278-6125(05)80019-6).
- [34] Sun Ch, Altintas Y. Chatter free tool orientations in 5-axis ball-end milling. *Int J Mach Tool Manuf* 2016;106:89–97. <https://doi.org/10.1016/j.ijmactools.2016.04.007>.